

Cross-section classification of elliptical hollow sections

L. Gardner[†] and T. M. Chan[‡]

*Department of Civil and Environmental Engineering, Imperial College London,
South Kensington Campus, London, SW7 2AZ, UK*

(Received November 14, 2005, Accepted January 22, 2007)

Abstract. Tubular construction is widely used in a range of civil and structural engineering applications. To date, the principal product range has comprised square, rectangular and circular hollow sections. However, hot-rolled structural steel elliptical hollow sections have been recently introduced and offer further choice to engineers and architects. Currently though, a lack of fundamental structural performance data and verified structural design guidance is inhibiting uptake. Of fundamental importance to structural metallic design is the concept of cross-section classification. This paper proposes slenderness parameters and a system of cross-section classification limits for elliptical hollow sections, developed on the basis of laboratory tests and numerical simulations. Four classes of cross-sections, namely Class 1 to 4 have been defined with limiting slenderness values. For the special case of elliptical hollow sections with an aspect ratio of unity, consistency with the slenderness limits for circular hollow sections in Eurocode 3 has been achieved. The proposed system of cross-section classification underpins the development of further design guidance for elliptical hollow sections.

Keywords: cross-section classification; elliptical hollow sections; laboratory testing; numerical modelling; oval hollow sections; rotation capacity; slenderness limits; steel structures.

1. Introduction

Elliptical hollow sections (EHS) combine the merits of traditional circular hollow sections (CHS) and sections with different major and minor axis properties such as rectangular hollow sections (RHS). The smooth streamlined shape is not only architecturally appealing but also favourable for reducing wind resistance. Examples of projects incorporating EHS include the coach station at Heathrow Terminal 3 in the UK, the Guadeloupe-Pôle-Caraïbes air terminal at Pointe-à-Pitre in France and the main railway station at Bern in Switzerland. Recent research on the behaviour and design of connections between EHS (Bortolotti *et al.* 2003, Choo *et al.* 2003, Pietrapertosa and Jaspart 2003, Willibald *et al.* 2006) and a tentative proposal on cross-section classification for EHS (Corus 2006) have highlighted the need for comprehensive structural design guidance. This paper proposes a cross-section classification system and section classification limits for elliptical hollow sections in compression and bending. The present research forms part of a wider study on the structural response of elliptical hollow sections.

[†]Lecturer, Corresponding author, E-mail: Leroy.gardner@imperial.ac.uk

[‡]Research student, E-mail: ken.chan@imperial.ac.uk

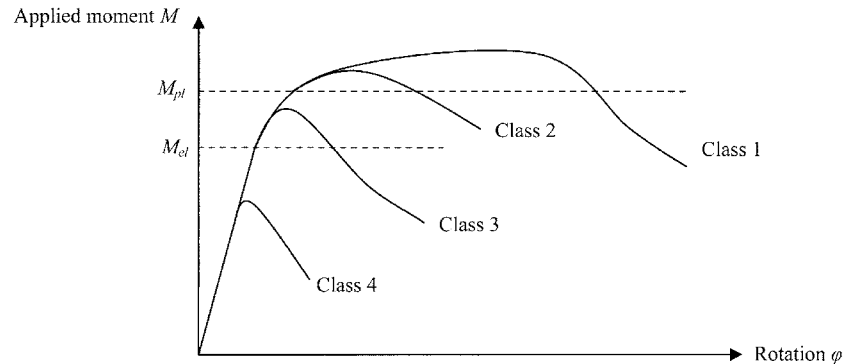


Fig. 1 Four behavioural classes of cross-section

2. Cross-section classification

The majority of structural steel design codes including Eurocode 3, place cross-sections into one of four behavioural classes based upon their susceptibility to local buckling. Class 1 cross-sections are capable of reaching and maintaining their full plastic moment in bending (and may therefore be used in plastic design). Sufficient deformation capacity or rotation capacity has to be demonstrated in this behavioural class. Class 2 cross-sections are also capable of reaching their full plastic moment in bending but have somewhat lower deformation capacity. In Class 3 cross-sections, local buckling prevents attainment of the full plastic moment and the bending moment resistance is limited to the yield (elastic) moment. For Class 4 cross-sections, local buckling occurs in the elastic range and bending resistance is determined on the basis of an effective cross-section defined by the width-to-thickness (or diameter-to-thickness) ratios of the constituent elements. The moment-rotation characteristics of the four behavioural classes are summarized in Fig. 1.

In this paper, Class 1 to 3 slenderness limits are determined on the basis of tests and verified by numerical models in three-point and four-point bending configurations. Limits are established for bending about both the major and minor axes, and validated against the CHS limits in EN 1993-1-1 (2005). Compression tests have been used to confirm the applicability of the Class 3 limit on the basis of whether or not the yield load is reached. Development of a method for the determination of effective section properties for Class 4 cross-sections is underway.

3. Rotation capacity

In plastic design, members must be capable of forming plastic hinges which allow rotation whilst sustaining the plastic moment resistance until a collapse mechanism is formed. The total rotation of the first plastic hinge to form in a collapse mechanism defines the required rotation capacity. Class 1 cross-sections must have sufficient rotation capacity to meet this requirement.

Rotation capacity can be determined by two commonly adopted methods. One is evaluated from the moment-curvature relationship and the other is based on the moment-rotation behaviour. The former method has been widely utilised in the literature (Korol and Hudoba, 1972 Hasan and Hancock 1989, Wilkinson and Hancock 1998, Jiao and Zhao 2004) to determine the rotation capacity of structural

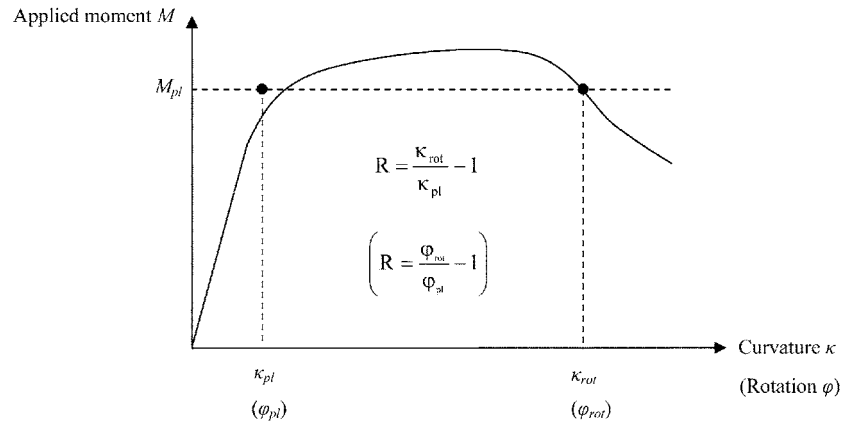


Fig. 2 Definition of rotation capacity from moment-curvature and moment-rotation graphs

hollow sections in a four-point bending arrangement. The rotation capacity R of a plastic hinge based on the moment-curvature relationship is defined by Eq. (1).

$$R = \frac{\kappa_{rot}}{\kappa_{pl}} - 1 \tag{1}$$

where κ_{pl} is evaluated as M_{pl}/EI , where M_{pl} is the plastic moment resistance, E is Young's modulus and I is the second moment of area, and κ_{rot} is the limiting curvature at which the moment resistance drops back below M_{pl} (Fig. 2).

Similarly, the definition of rotation capacity based on the moment-rotation relationship (Fig. 2) has been commonly used in the literature (Strangh ner *et al.* 1994, Rondal *et al.* 1995, Sedlacek and Feldmann 1995, Gioncu *et al.* 1996, Sedlacek *et al.* 1998), and is given by Eq. (2)

$$R = \frac{\varphi_{rot}}{\varphi_{pl}} - 1 \tag{2}$$

where φ_{pl} is the elastic component of rotation upon reaching M_{pl} and φ_{rot} is the limiting rotation at which the moment resistance falls back below M_{pl} .

In the current study, both four-point bending and three-point bending testing arrangements have been employed; the four-point bending configuration enables the study of the cross-section behaviour under uniform moment with negligible influence from shear. The former definition of rotation capacity based on the moment-curvature relationship was therefore adopted for evaluating the four-point bending test and numerical results. The three-point bending arrangement allows study of the cross-section behaviour under a moment gradient and in the presence of shear, and in this case the moment-rotation relationship was used to evaluate rotation capacity from the test and numerical results.

A number of studies have been conducted to determine the required level of rotation capacity to allow sufficient moment redistribution in plastic design. By considering plastic collapse mechanisms in a variety of frames and multi-span beams, required values of rotation capacity R of 3 (adopted by Yura *et al.* 1978, Strangh ner *et al.* 1994, Rondal *et al.* 1995, Sedlacek and Feldmann 1995, Sedlacek *et al.* 1998, Jiao and Zhao 2004) and 4 (adopted by Korol and Hudoba 1972, Hasan and Hancock 1989, Wilkinson and Hancock 1998, Jiao and Zhao 2004) have been proposed. A rotation capacity R of 3 was adopted in the development of the current European (EN 1993-1-1, 2005) and North American (AISC,

2005a and 2005b) steel design codes. Likewise, a value of rotation capacity of 3 has been assumed for the development of the Class 1 classification limit in this paper.

4. Laboratory testing

4.1 Imperial College London tests

As part of a major research programme at Imperial College London, a series of full-scale laboratory tests on elliptical hollow sections (grade S355) was performed to generate fundamental structural performance data. The test programme comprised a total of 25 tensile coupon tests, 25 stub column tests, 8 three-point bending tests (4 about the major axis and 4 about the minor axis) and 10 four-point bending tests (3 about the major axis and 7 about the minor axis). The primary objective of the tensile coupon tests was to determine the basic engineering stress-strain behaviour of the material for each of the tested section sizes. Results were used to facilitate the numerical study described in Section 5. Cross-section capacity stub column tests and in-plane bending tests were conducted to develop a relationship between cross-section slenderness, deformation capacity and load-carrying capacity for elliptical hollow sections under (1) uniform axial compression, (2) uniform bending and (3) a moment gradient. Full load-end shortening curves were recorded, including into the post-ultimate range for stub column tests whilst full moment-rotation curves and moment-curvature curves were derived, including into the post-ultimate range for three-point and four-point bending tests respectively. Full details of the test arrangements and results have been reported by Chan and Gardner (In press) and Chan and Gardner (Submitted), whilst a summary of the initial tests was reported by Gardner and Ministro (2005).

4.2 University of Southampton tests

An experimental study of the minor axis bending behaviour of structural EHS was conducted at the University of Southampton (Eckhardt 2004). The in-plane minor axis bending tests were conducted in a symmetrical four-point bending arrangement. Moment-rotation behaviour was recorded during the tests but not into the unloading regime. It is therefore not clear that the ultimate moment resistance was reached, and it was not possible to determine rotation capacity.

5. Numerical simulations

5.1 General

A numerical modelling programme, using the finite element (FE) package ABAQUS (2006), was carried out in parallel with the experimental programme. The primary objectives of the programme were to replicate the experimental compression and bending behaviour numerically and, having validated the models, to perform parametric studies. The elements chosen for the FE models were 4-noded, reduced integration shell elements, designated as S4R in the ABAQUS element library, and suitable for thin or thick shell applications (ABAQUS 2006). Convergence studies were conducted to decide upon an appropriate mesh density, with the aim of achieving suitably accurate results whilst minimising computational time. Satisfactory results were obtained using uniform mesh densities

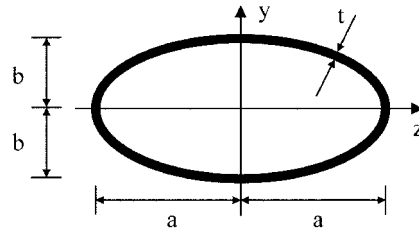


Fig. 3 Geometry of an elliptical hollow section

throughout the models.

The tests were modelled using the measured dimensions of the test specimens and material stress-strain data from the corresponding tensile coupon tests. Geometric imperfections took the form of the lowest elastic buckling modes. The imperfection amplitude was considered as three fixed fractions of the material thickness t ($t/10$, $t/100$ and $t/500$) in addition to the measured imperfection values. For beam tests, a nominal global imperfection amplitude or geometrical ‘out of straightness’ of $L/500$ (EN 10210-2, 2006) where L is the specimen length was employed throughout. No residual stress data were measured, but negligible deformation observed when the material tensile coupons were machined from the elliptical specimens indicated that the residual stress were low. Therefore, residual stresses were not incorporated into the numerical models in this study. The true stress-strain relations were generated from the engineering stress-strain curves obtained from the tensile coupon tests and material non-linearity was incorporated into the numerical models by means of a piecewise linear stress-strain model to mimic, in particular, the strain-hardening region. The modified Riks method (ABAQUS 2006) was employed to solve the geometrically and materially non-linear models, which enabled the unloading behaviour to be traced.

Following satisfactory agreement between test and FE model behaviour, parametric studies on cross-section slenderness were conducted. The primary objectives of the parametric studies were to investigate the influence of cross-section slenderness and aspect ratio on the ultimate load carrying capacity and deformation capacity, to analyse trends and to enlarge the population of results. Aspect ratios a/b of 1 (CHS), 2 and 3 were studied, where a and b are defined in Fig. 3. Material thickness was varied in order to cover a spectrum of cross-section slenderness. The results have been utilized for the validation of proposed slenderness parameters and cross-section classification limits for elliptical hollow sections and are discussed in detail in the following section. Further modelling details and numerical results have been reported by Chan and Gardner (In press) and Chan and Gardner (Submitted).

6. Definition of cross-section slenderness

The elastic critical buckling stress σ_{cr} of a uniformly compressed oval shell may be closely approximated by substituting the expression for the maximum radius of curvature r_{\max} into the classical buckling stress of a circular cylinder (Kemper 1962), as given by Eq. (3).

$$\sigma_{cr} = \frac{E}{\sqrt{3(1-\nu^2)}(r_{\max}/t)} \quad (3)$$

where E is the Young's modulus, ν is Poisson's ratio and t is the thickness of the shell. This assumes that buckling initiates at the point of maximum radius of curvature and ignores the restraining effect of the surrounding material of lower radius of curvature. This approximation provides a lower bound solution to the critical buckling stress of an oval section.

For an elliptical section, the maximum radius of curvature occurs at the end of the cross-section major (y - y) axis, and may be shown to be equal to a^2/b . Thus, the elastic critical buckling stress for an elliptical cylinder may be approximated by Eq. (4).

$$\sigma_{cr} = \frac{E}{\sqrt{3(1-\nu^2)}(a^2/bt)} \quad (4)$$

Note that for the case where $a = b$, Eq. (4) reverts exactly to the elastic critical buckling stress of a circular cylinder, whilst for high a/b ratios the critical buckling stress approaches that predicted by the classical buckling expression for a flat plate.

With reference to Eq. (4), it is therefore proposed that under compression and bending about the minor axis, the cross-section slenderness of an elliptical hollow section is defined as

$$\frac{D_e}{t\epsilon^2} = 2\frac{(a^2/b)}{t\epsilon^2} \quad (5)$$

where D_e is the equivalent diameter and $\epsilon^2 = 235/f_y$ to allow for a range of yield strengths.

For bending about the major axis, buckling would initiate in general neither at the point of maximum radius of curvature (located at the neutral axis of the cross-section with negligible bending stress) nor at the extreme of the major axis (where the maximum compressive stress occurs). Gerard and Becker (1957) suggested that in this bending situation, determination of the elastic buckling stress involves the location of a point of critical curvature. This critical radius of curvature r_{cr} was calculated by optimizing the function composed of the varying curvature expression and the elastic bending stress distribution and was found to be equal to $0.65 a^2/b$ (Fig. 4). For an aspect ratio a/b of less than 1.155, where the section is approaching circular, Gerard and Becker (1957) observed that buckling would occur at the extreme of the major axis and that r_{cr} would therefore be equal to a . However, at the extreme of the

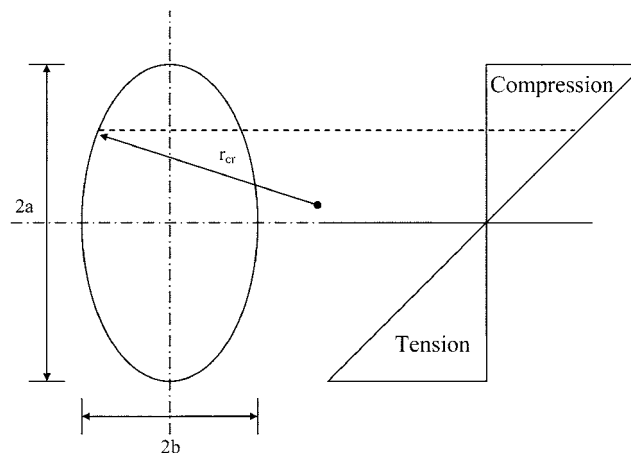


Fig. 4 Location of critical radius of curvature in elastic major axis bending

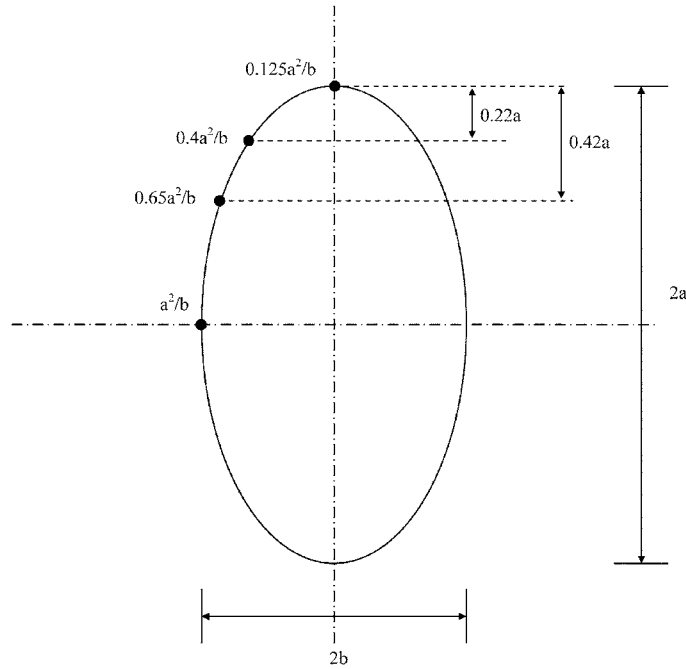


Fig. 5 Radius of curvature at different positions (aspect ratio $a/b=2$)

major axis, the radius of curvature is, in fact, equal to b^2/a . For a/b less than 1.155, r_{cr} has therefore been taken as b^2/a herein.

As described above, for an elliptical hollow section in major axis bending with an aspect ratio a/b of 2, elastic critical buckling would initiate, theoretically, at a distance $0.42a$ ($r = 0.65a^2/b$) from the extreme fibre in compression. However, from the experimental results, use of the radius at a distance of $0.22a$ ($r = 0.4a^2/b$) from the extreme compressive fibre more closely reflects the observed physical behaviour (see Fig. 5).

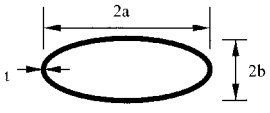
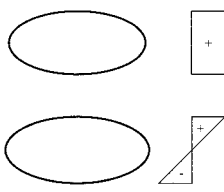
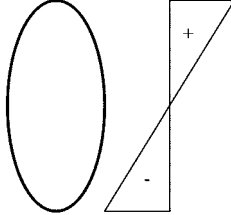
Thus, for a general slenderness parameter in major axis bending for the cross-section classification of EHS, it is proposed to utilize the findings of Gerard and Becker (1957) based on an elastic stress distribution, with modification based on observed physical behaviour. The proposed slenderness parameters are therefore given by Eq. (6) and Eq. (7).

$$\frac{D_e}{t\varepsilon^2} = 0.8 \frac{(a^2/b)}{t\varepsilon^2} \quad \text{for } a/b > 1.155 \quad (6)$$

$$\frac{D_e}{t\varepsilon^2} = 2 \frac{(b^2/a)}{t\varepsilon^2} \quad \text{for } a/b \leq 1.155 \quad (7)$$

Note that for the special case of an EHS with an aspect ratio of unity, the cross-section slenderness defined by Eq. (7) reverts to that for CHS in Eurocode 3. A summary of the proposed cross-section slenderness parameters for EHS are summarised in Table 1.

Table 1 Cross-section slenderness

	
Cross-section slenderness $\frac{D_e}{t\epsilon^2}$	
Compression / Bending about minor axis	Bending about major axis
$2\left(\frac{a^2}{b}\right)/t\epsilon^2$	$0.8\left(\frac{a^2}{b}\right)/t\epsilon^2$ for $a/b > 1.155$
	$2\left(\frac{b^2}{a}\right)/t\epsilon^2$ for $a/b \leq 1.155$
	
Note: $\epsilon^2 = 235/f_y$	

7. Cross-section classification

7.1 General

On the basis of the aforementioned slenderness parameters, all experimental results for EHS have been plotted in Figs. 6-12. Fig. 6 summarises the behaviour of EHS in compression, whilst bending behaviour about the two principal axes is depicted in Figs. 7-12.

For comparison, existing compressive test data from CHS have also been added to Fig. 6. Due to the

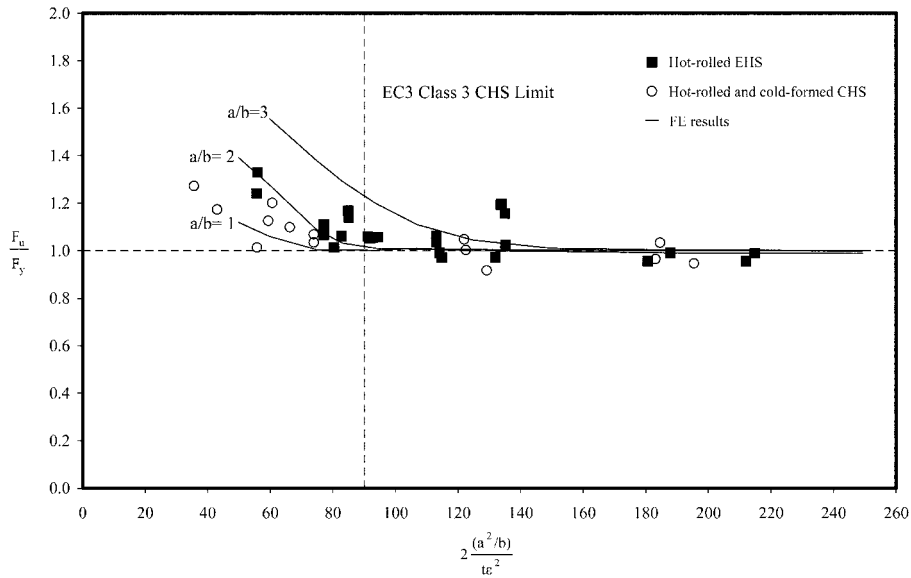


Fig. 6 F_u/F_y versus cross-section slenderness

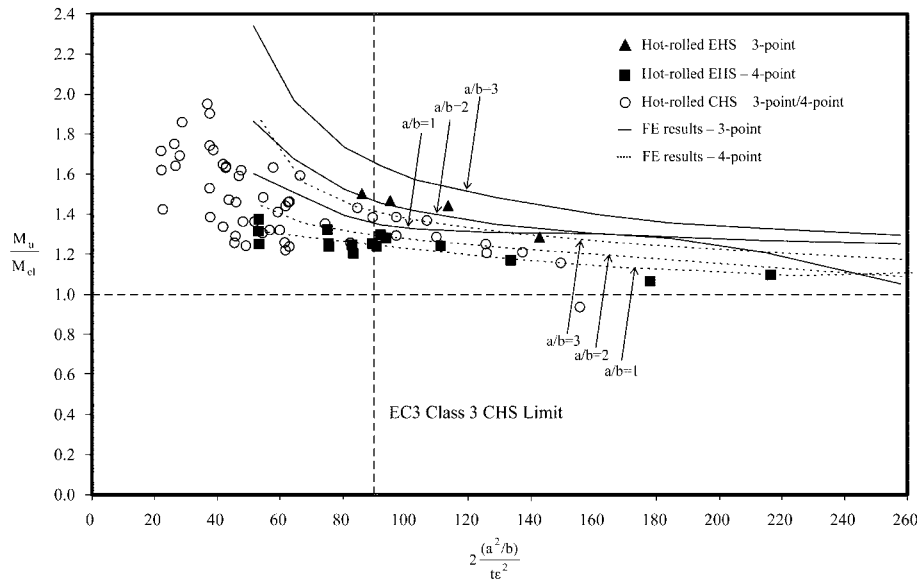
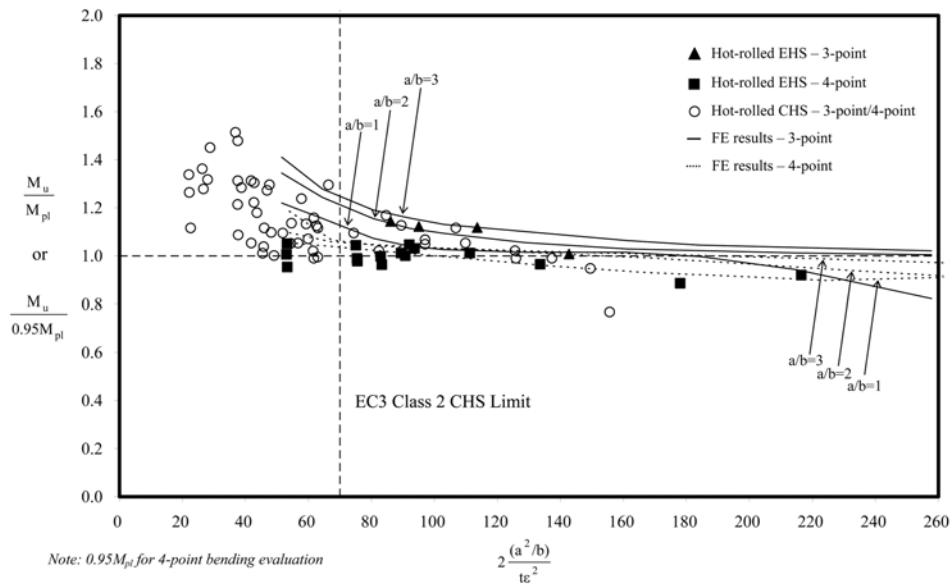


Fig. 7 M_u/M_{el} versus cross-section slenderness (minor axis bending)



Note: $0.95M_{pl}$ for 4-point bending evaluation

Fig. 8 M_u/M_{pl} or $M_u/0.95 M_{pl}$ versus cross-section slenderness (minor axis bending)

limited number of hot-rolled CHS data available, both hot-rolled (Giakoumelis and Lam 2004, Teng and Hu 2007) and cold-formed (Sakino *et al.* 2004, Tutuncu and O'Rourke 2006) CHS data have been included.

Similarly, to compare EHS with CHS in bending, experimental results of the flexural behaviour of hot-rolled steel CHS (Schilling 1965, Jirsa *et al.* 1972, Sherman 1976, 1986, Rondal *et al.* 1995, Sedlacek *et al.* 1998) have also been included in Figs. 7-12. It should be stated that the experimental

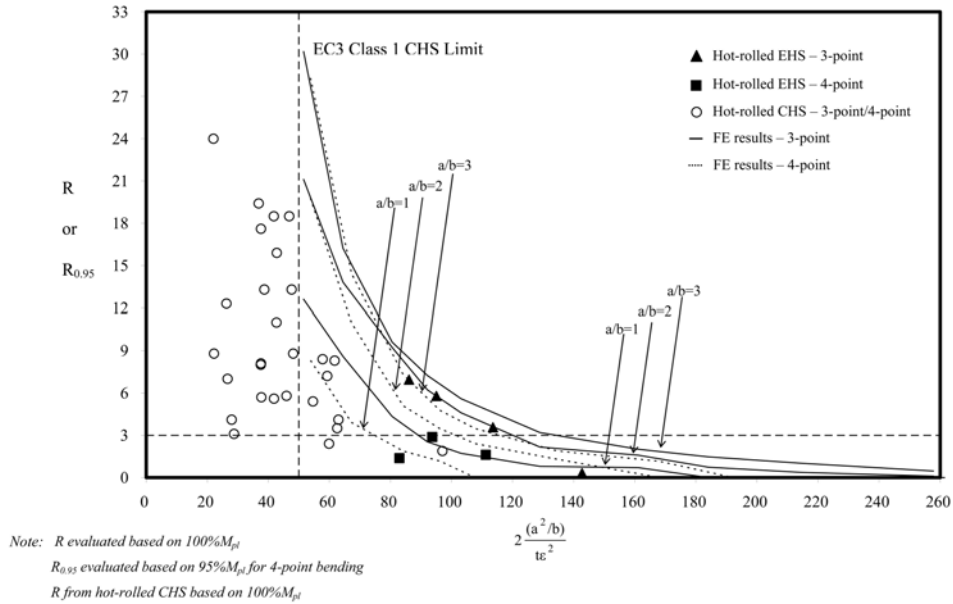


Fig. 9 Rotation capacity versus cross-section slenderness (minor axis bending)

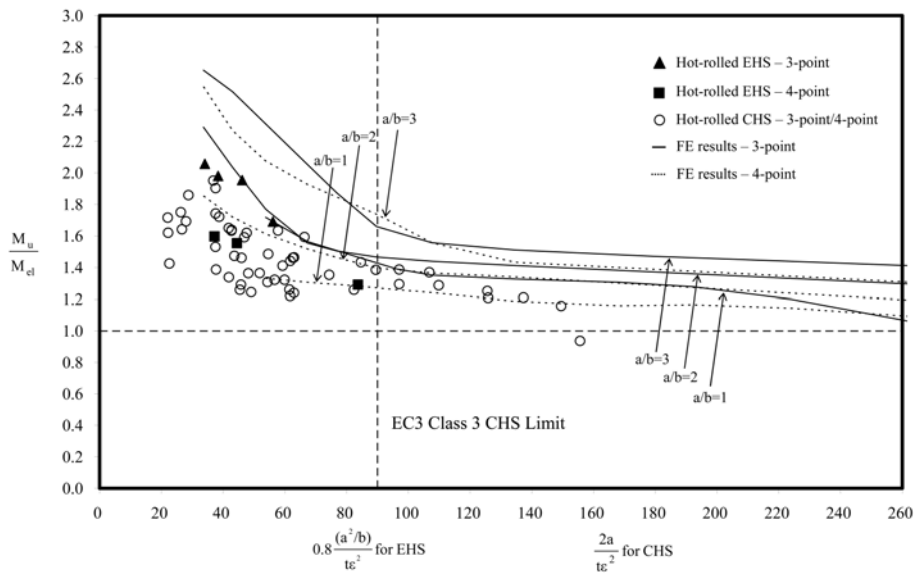


Fig. 10 M_u/M_{el} versus cross-section slenderness (major axis bending)

research from Schilling (1965), Jirsa *et al.* (1972) and Sherman (1976, 1986) formed the basis for the system of cross-section classification of the current North American (AISC, 2005a) steel design code; the research work from Rondal *et al.* (1995) and Sedlacek *et al.* (1998) underpins the European (EN 1993-1-1, 2005) limits.

Results are considered in more detail in the following sections, though it may generally be observed that, on the basis of the proposed slenderness parameters, the EHS and CHS data follow similar trends. This suggests that the CHS limits in EN 1993-1-1 (2005) may also be safely applied to EHS (adopting

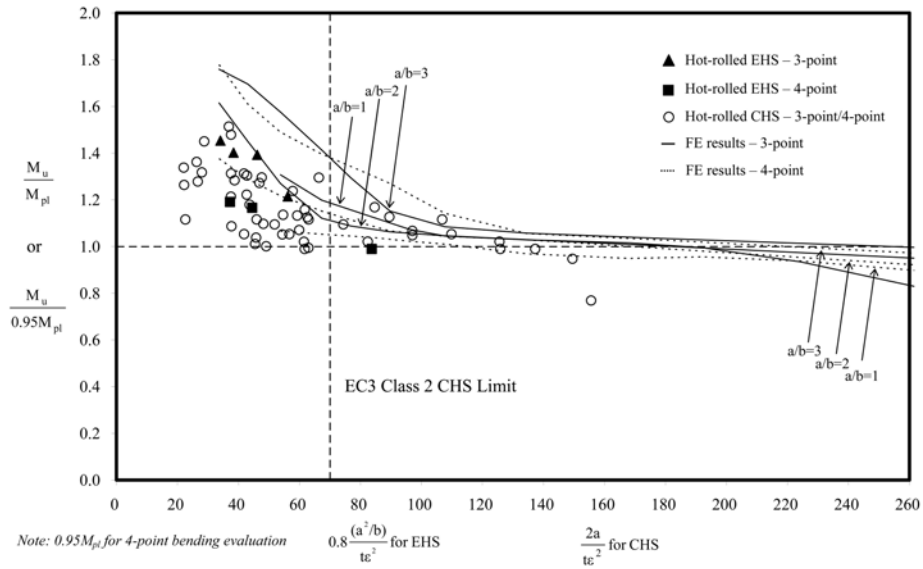


Fig. 11 M_u/M_{pl} versus cross-section slenderness (major axis bending)

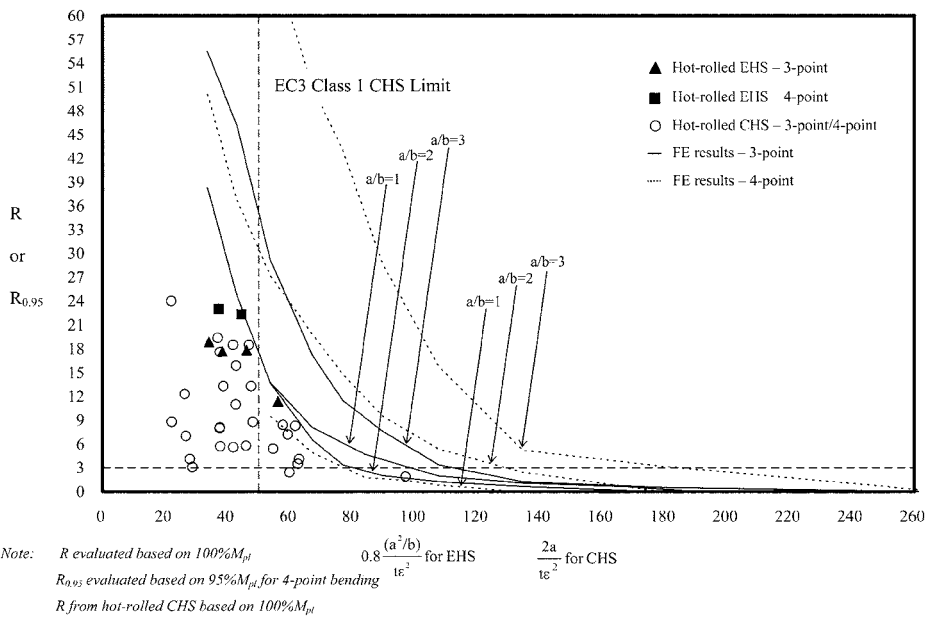


Fig. 12 Rotation capacity versus cross-section slenderness (major axis bending)

the proposed measures of slenderness); though the data reveals that relaxation of the limits for both section types may be appropriate. It is worth noting that the current classification limits given in EN 1993-1-1 (2005) and AISC (2005a) are clearly sensitive to the range of data upon which they were developed; this will be further discussed, together with the proposed cross-section classification limits for EHS in the following sections.

7.2 Compression

Axial compression represents one of the fundamental loading arrangements for structural members. For cross-section classification under pure compression, of primary concern is the occurrence of local buckling in the elastic material range (i.e. below the yield stress). Cross-sections that reach the yield load are considered Class 1-3, Eq. (8), whilst those where local buckling of the slender constituent elements prevents attainment of the yield load are Class 4. Local buckling is accounted for in Class 4 cross-sections through the effective area concept, Eq. (9).

$$N_{c,Rd} = Af_y / \gamma_{M0} \quad (\text{Class 1-3}) \quad (8)$$

$$N_{c,Rd} = A_{eff}f_y / \gamma_{M0} \quad (\text{Class 4}) \quad (9)$$

where A is the gross cross-sectional area, A_{eff} is the effective area, f_y is the material yield strength and γ_{M0} is a partial factor for cross-section resistance, generally taken equal to unity.

Development of a method for the determination of effective section properties for Class 4 elliptical hollow sections is underway.

Results from the stub columns tests conducted at Imperial College London are summarised in Fig. 6. In this figure, the ultimate test load F_u has been normalised by the yield load F_y (defined as the yield strength f_y multiplied by the gross cross-sectional area), and the relationship between F_u/F_y and cross-section slenderness $2(a^2/b)/t\varepsilon^2$ has been plotted. A value of F_u/F_y greater than unity represents meeting of the Class 1-3 requirement, whilst a value less than unity indicates a Class 4 cross-section where local buckling prevents the yield load from being reached. Fig. 6 exhibits the anticipated trend of reducing values of F_u/F_y with increasing slenderness. A lower bound to the test results suggests that the CHS Class 3 slenderness limit of 90 from EN 1993-1-1 (2005) may also be applied to EHS. In addition to experimental results, results from the parametric studies for EHS with aspect ratios a/b of 1, 2 and 3 have also been plotted; these results support the appropriateness of adopting the Class 3 CHS limit from EN 1993-1-1 (2005).

7.3 Bending

For cross-section classification in bending, distinction is made between cross-sections depending on their rotation capacity and their ability to reach the plastic and elastic moment resistances, as indicated by Eqs. (10) to (13). The following sub-sections compare the test results with the four cross-section class requirements under two loading configurations: four-point bending (where the member is subjected to uniform moment) and three-point bending (where the member is subjected to a moment gradient).

$$M_{c,Rd} = W_{pl}f_y / \gamma_{M0} \text{ and } R > 3 \quad (\text{Class 1}) \quad (10)$$

$$M_{c,Rd} = W_{pl}f_y / \gamma_{M0} \quad (\text{Class 2}) \quad (11)$$

$$M_{c,Rd} = W_{el}f_y / \gamma_{M0} \quad (\text{Class 3}) \quad (12)$$

$$M_{c,Rd} = W_{eff}f_y / \gamma_{M0} \quad (\text{Class 4}) \quad (13)$$

where W_{pl} is the plastic section modulus, W_{el} is the elastic section modulus and W_{eff} is the effective section modulus, which is currently under investigation.

The behaviour of beams under uniform bending differs from that under a moment gradient (Galambos

1968, Gioncu *et al.* 1996): Under uniform bending, the bending moment remains constant (along a moment plateau) until the average outer fibre strain reaches the strain hardening strain ε_{sh} along the entire uniform moment length. Only then may the bending moment rise above M_{pl} . Many tests (Lay and Galambos 1965, Sedlacek *et al.* 1998) and the numerical simulations have demonstrated that the moment plateau occurs below M_{pl} and thus the definition of rotation capacity (Eq. 1) is not appropriate. Conversely, for beam under a moment gradient, the plastic hinge is localized and strain-hardening occurs as soon as M_{pl} is reached. The moment will continue to increase until the yielded length of the compression flange is equal to the full local buckling wavelength (Galambos 1968).

To take account of this phenomenon, researchers (Lay and Galambos 1965, Sedlacek *et al.* 1998) have suggested that for beams with uniform bending moment, the rotation capacity should be determined at a reduced plastic moment $0.95 M_{pl}$. Thus rotation capacity $R_{0.95}$ is defined by Eq. (14)

$$R_{0.95} = \frac{\kappa_{rot, 0.95}}{\kappa_{pl, 0.95}} - 1 \quad (14)$$

This definition is used throughout this paper for beams in the four-point bending arrangement.

7.3.1 Minor axis bending

Fig. 7 shows the relationship between minor axis moment resistance and the proposed cross-section slenderness. In this figure, the ultimate test moment M_u has been normalised by the elastic moment resistance M_{el} , and plotted against cross-section slenderness $2(a^2/b)/t\varepsilon^2$. A value of M_u/M_{el} greater than unity represents meeting of the Class 3 requirement, whilst a value less than unity indicates a Class 4 cross-section where local buckling prevents the yield moment being reached. A lower bound to the experimental results suggests that the Eurocode limit of 90 representing the boundary between Class 3 and 4 cross-sections may be safely adopted. In addition to experimental results, results from the numerical parametric studies on EHS with aspect ratios a/b of 1, 2 and 3 have also been plotted and again, these indicate the appropriateness of adopting the Class 3 CHS limit from EN 1993-1-1 (2005). It is worth noting that the Eurocode Class 3 slenderness limit of 90 for CHS in bending was derived on the basis of the trend from tests on stocky cross-sections made by Rondal *et al.* (1995) and Sedlacek *et al.* (1998), whilst Schilling (1965), Jirsa *et al.* (1972) and Sherman (1976, 1986) tested sections with a wider range of slenderness and derived the less strict value for the Class 3 limit that has been adopted in AISC (2005a). This demonstrates that classification limits can be sensitive to the slenderness range of test data upon which they are developed.

The ultimate moments attained in the tests have also been normalised against the plastic moment resistance (M_{pl} for three-point bending and $0.95 M_{pl}$ for four-point bending) and plotted against cross-section slenderness $2(a^2/b)/t\varepsilon^2$ in Fig. 8. A value of $M_u/0.95 M_{pl}$ or M_u/M_{pl} greater than unity represents meeting of the Class 2 requirement, while a value less than unity indicates a Class 3 or 4 section where local buckling prevents attainment of the full plastic moment. The data generally indicate that the EN 1993-1-1 (2005) Class 2 limit may be safely adopted. This is further evidenced by the parametric results on EHS with aspect ratios of 1, 2 and 3. It is worth noting that the three stockiest experimental points relate to the tests described by Eckhardt (2004) where the ultimate moment resistance was not reached.

Both Class 1 and Class 2 cross-sections are capable of reaching their plastic bending moment resistance ($0.95 M_{pl}$ for four-point bending and M_{pl} for three-point bending). Distinction between these two classes is made on the basis of rotation capacity R . Fig. 9 plots rotation capacity (as defined by Eq. (1), Eq. (2) and Eq. (14)) against cross-section slenderness. As discussed earlier, a rotation capacity R of 3 is required for a Class 1 cross-section. From a lower bound analysis of the test data a Class 1 classification limit of 50 from

EN 1993-1-1 (2005) may be safely adopted. Detailed analysis of the test and numerical results from the three-point and four-point bending arrangements has been reported by Chan and Gardner (Submitted).

7.3.2 Major axis bending

Results of experiments in four-point and three-point bending about the major axis, complemented by the numerical parametric results, have been plotted in Figs. 10 to 12 based on the proposed slenderness parameters of Table 1. The results show similar trends to the case of minor axis bending indicating that the Eurocode limits applied to CHS may be safely adopted for EHS, using the proposed slenderness parameters. Fig. 12 shows that although the EHS exhibit greater rotation capacity at low slenderness, results converge towards those for CHS at the required rotation capacity of 3.

It may be seen from the results in compression, minor axis bending and major axis bending that, using the proposed slenderness parameters for EHS, the Eurocode classification limits for CHS may be safely adopted. Further analysis of the results indicates that the Class 3 slenderness limit for both CHS and EHS (bending about either axis) may be relaxed to $140\epsilon^2$.

7.4 Combined compression and bending

For cross-section classification under combined compression and bending, designers can initially check the cross-section against the most severe loading case of pure compression. If the classification is Class 1, then there is no benefit to be gained from checking against the actual stress distribution. Similarly, if plastic design is not being utilized, there would be no benefit in re-classifying a Class 2 cross-section under the actual stress distribution. Under combined compression and minor axis bending, clearly buckling will initiate in the region of the maximum radius of curvature, similar to the case of pure compression and pure minor axis bending. Hence, for this case, the same slenderness parameter and classification limits are recommended. Under combined compression and major axis bending, the critical radius of curvature will shift towards the centroidal axis. Conservatively, classification may be carried out assuming pure compression, though development of a method for determination of the critical radius of curvature and the corresponding slenderness parameters and limits is currently underway.

8. Conclusions

Cross-section classification is a fundamental aspect of structural metallic design. This paper has proposed slenderness parameters and a system of cross-section classification limits for elliptical hollow sections in compression, bending about both principal axes and combined compression plus bending. Compatibility with CHS limits has been achieved. The results demonstrate that, using the proposed measures of slenderness for EHS, the Eurocode 3 cross-section classification limits for CHS may be safely adopted. Proposals for improved limits have also been made. The developed classification system underpins the development of further structural design guidance for elliptical hollow sections.

Acknowledgements

The authors are grateful to the Dorothy Hodgkin Postgraduate Award Scheme for the project funding, and would like to thank Corus for the supply of test specimens and for funding contributions, Eddie

Hole and Andrew Orton (Corus Tubes) for their technical input and Ron Millward, Alan Roberts and Trevor Stickland (Imperial College London) for their assistance in the laboratory works.

References

- ABAQUS (2006), *ABAQUS/Standard User's Manual Volumes I-III and ABAQUS CAE Manual. Version 6.6.* Hibbit, Karlsson & Sorensen, Inc. Pawtucket, USA.
- AISC (2005a), *Specification for Structural Steel Buildings*, American Institute of Steel Construction, Chicago.
- AISC (2005b), *Commentary on the Specification for Structural Steel Buildings*, American Institute of Steel Construction, Chicago.
- Bortolotti, E., Jaspart, J. P., Pietrapertosa, C., Nicaud, G., Petitjean, P. D. and Grimault, J. P. (2003), "Testing and modelling of welded joints between elliptical hollow sections", *Proceedings of the 10th International Symposium on Tubular Structures*, Madrid, September.
- Chan, T. M. and Gardner, L. (In press), "Compressive resistance of hot-rolled elliptical hollow sections", *Eng. Struct.*
- Chan, T. M. and Gardner, L. (Submitted), "Bending strength of hot-rolled elliptical hollow sections", *J. Struct. Eng.*, ASCE.
- Choo, Y. S., Liang, J. X. and Lim, L. V. (2003), "Static strength of elliptical hollow section x-joint under brace compression", *Proceedings of the 10th International Symposium on Tubular Structures*, Madrid, September.
- Corus (2006), *Celsius[®] 355 Ovals – Sizes and Resistances Eurocode Version*, Corus Tubes – Structural & Conveyance Business.
- Eckhardt, C. (2004), *Classification of oval hollow sections*. University of Southampton.
- EN 1993-1-1 (2005), *Eurocode 3: Design of steel structures – Part 1-1: General rules and rules for buildings*, CEN.
- EN 10210-2 (2006), *Hot finished structural hollow sections of non-alloy and fine grain steels – Part 2: Tolerances, dimensions and sectional properties*, CEN.
- Galambos, T. V. (1968), "Deformation and energy absorption capacity of steel structures in the inelastic range", *American Iron and Steel Institute, Bulletin No. 8*
- Gardner, L. and Ministro, A. (2005), "Structural steel oval hollow sections", *The Structural Engineer*, **83**(21), 32-36.
- Gerard, G. and Becker, H. (1957), *Handbook of structural stability: Part III – Buckling of curved plates and shells*, NACA TN-3783.
- Giakoumelis, G. and Lam, D. (2004), "Axial capacity of circular concrete-filled tube columns", *J. Constr. Steel Res.*, **60**(7), 1049-1068.
- Gioncu, V., Tircă, L. and Petcu, D. (1996), "Rotation capacity of rectangular hollow section beams", *Proceedings of the 7th International Symposium on Tubular Structures*, Miskolc, August.
- Hasan, S. W. and Hancock, G. J. (1989), "Plastic bending tests of cold-formed rectangular hollow sections", *Steel Construction*, Australian Steel Institute, **23**(4), 2-19.
- Jiao, H. and Zhao, X. L. (2004), "Section slenderness limits of very high strength circular steel tubes in bending", *Thin-Walled Structures*, **42**(9), 1257-1271.
- Jirsa, J. O., Lee, F. H., Wilhoit, J. C. and Merwin, J. E. (1972), "Ovaling of pipelines under pure bending", *Proceedings of the 4th Offshore Technology Conference*, Houston, May.
- Kempner, J. (1962), "Some results on buckling and postbuckling of cylindrical shells", *Collected Papers on Instability Shell Structures*, NASA TN D-1510, 173-186.
- Korol, R. M. and Hudoba, J. (1972), "Plastic behavior of hollow structural sections", *J. Struct. Div.*, ASCE, **98**(5), 1007-1023.
- Lay, M. G. and Galambos, T. V. (1965), "Inelastic steel beams under uniform moment", *J. Struct. Div.*, ASCE, **91**(6), 67-93.
- Pietrapertosa, C. and Jaspart, J. P. (2003), "Study of the behaviour of welded joints composed of elliptical hollow sections", *Proceedings of the 10th International Symposium on Tubular Structures*, Madrid, September.
- Rondal, J., Boeraeve, Ph., Sedlacek, G., Stranghöner, N. and Langenberg, P. (1995), *Rotation Capacity of Hollow Beam Sections*, CIDECT.

- Sakino, K., Nakahara, H., Morina, S. and Nishiyama, I. (2004), "Behavior of centrally loaded concrete-filled steel-tube short columns", *J. Struct. Eng.*, ASCE, **130**(2), 180-188.
- Schilling, C. G. (1965). "Buckling strength of circular tubes", *J. Struct. Div.*, ASCE, **91**(5), 325-348.
- Sedlacek, G., Dahl, W., Strangh ner, N., Kalinowski, B., Rondal, J. and Boraev, Ph. (1998), "Investigation of the rotation behaviour of hollow section beams", EUR 17994 EN, European Commission.
- Sedlacek, G. and Feldmann, M. (1995), Background document 5.09 for chapter 5 of Eurocode 3 Part 1.1 – The *b/t* ratios controlling the applicability of analysis models in Eurocode 3 Part 1.1, Aachen.
- Sherman, D. R. (1976), "Tests of circular steel tubes in bending", *J. Struct. Div.*, ASCE, **102**(11), 2181-2195.
- Sherman, D. R. (1986), "Inelastic flexural buckling of cylinders", *Proceedings of the Steel Structures: Recent Research Advances and Their Applications to Design*, Budva, September.
- Strangh ner, N., Sedlacek, G. and Boeraev, Ph. (1994), "Rotation requirement and rotation capacity of rectangular, square and circular hollow section beams", *Proceedings of the 6th International Symposium on Tubular Structures*, Melbourne, December.
- Teng, J. G. and Hu, Y. M. (2007), "Behaviour of FRP-jacketed circular steel tubes and cylindrical shells under axial compression", *Construction Building Materials*, **21**(4), 827-838.
- Tutuncu, I. and O'Rourke, T. D. (2006), "Compression behavior of non-slender cylindrical steel members with small and large-scale geometric imperfections", *J. Struct. Eng.*, ASCE, **132**(8), 1234-1241.
- Willibald, S., Packer, J. A. and Martinez-Saucedo, G. (2006), "Behaviour of gusset plate connections to ends of round and elliptical hollow structural section members", *Canadian J. Civil Eng.*, **33**(4), 373-383.
- Wilkinson, T. and Hancock, G. J. (1998), "Tests to examine compact web slenderness of cold-formed RHS", *J. Struct. Eng.*, ASCE, **124**(10), 1166-1174.
- Yura, J. A., Galambos, T. V. and Ravindra, M. K. (1978), "The bending resistance of steel beams", *J. Struct. Div.*, ASCE, **104**(9), 1355-1370.